Vibrational Analysis of the $\tilde{A}^2\Pi-\tilde{X}^2\Sigma^+$ and $\tilde{A}'^2\Delta-\tilde{X}^2\Sigma^+$ Transitions of BaOH and BaOD

W. T. M. L. FERNANDO, M. DOUAY,[1] AND P. F. BERNATH[2]

Department of Chemistry, University of Arizona, Tucson, Arizona 85721

The $\tilde{A}^2\Pi-\tilde{X}^2\Sigma^+$ transition of BaOH and BaOD was studied at low resolution by laser spectroscopy. The $\tilde{A}'^2\Delta-\tilde{X}^2\Sigma^+$ transition was also identified in the spectra. The $\tilde{A}^2\Pi$ state is perturbed by the $\tilde{B}^2\Sigma^+$ and $\tilde{A}'^2\Delta$ states. Ba–O stretching and Ba–O–H bending frequencies are extracted from the spectra. © 1990 Academic Press, Inc.

INTRODUCTION

In the course of our analysis of the $\tilde{B}^2\Sigma^+-\tilde{X}^2\Sigma^+$ transition of BaOH (*1*), we observed what we believed was the $\tilde{A}^2\Pi-\tilde{X}^2\Sigma^+$ transition by $\tilde{B}-\tilde{A}-\tilde{X}$ cascade emission. Unfortunately, this $\tilde{A}^2\Pi-\tilde{X}^2\Sigma^+$ analysis of BaOH was in error. We present here a vibrational analysis of the perturbed $\tilde{A}^2\Pi-\tilde{X}^2\Sigma^+$ transition observed directly by laser excitation spectroscopy and dispersed laser-induced fluorescence. The $\tilde{A}^2\Pi-\tilde{X}^2\Sigma^+$ transition of other alkaline earth metal monohydroxides, CaOH (*2, 3*) and SrOH (*4, 5*), has been analyzed at high resolution.

The $\tilde{A}^2\Pi$ and the $\tilde{B}^2\Sigma^+$ states are the only experimentally known low-lying electronic states for alkaline earth monohydroxides. However, for barium monohalides (*6, 8*) and monohydrides (*9, 10*) there is a low-lying $A'^2\Delta$ state with the B, A and A' states forming a *d*-complex. Martin and Royen discovered the $A'^2\Delta$ state in BaCl (*6*). More recently high-resolution infrared Fourier transform emission spectra recorded by laser excitation to the $C^2\Pi$ states of BaI (*7*) and BaF (*8*) yield $C^2\Pi-A'^2\Delta$ fluorescence. The discovery of the $A'^2\Delta$ state for BaF suggests that the lowest-lying excited electronic state for the isoelectronic BaOH is also $\tilde{A}'^2\Delta$. Our BaOH and BaOD spectra show evidence of the nominally forbidden $A'^2\Delta-\tilde{X}^2\Sigma^+$ transition.

The $\tilde{A}^2\Pi-\tilde{X}^2\Sigma^+$ transition of BaOH and BaOD occur in the 8000–9000 Å region of the spectrum. The $\tilde{A}^2\Pi$ state is badly perturbed by the $\tilde{B}^2\Sigma^+$ and $\tilde{A}'^2\Delta$ states, and the Renner–Teller effect complicates the vibronic structure. We are not, therefore, completely happy with our assignments and many bands remain unassigned. We are publishing our bandhead analysis to correct our previous erroneous $\tilde{A}-\tilde{X}$ assignments and as an aid to workers interested in the dynamics of the Ba + H$_2$O reaction (*11*).

EXPERIMENTAL DETAILS

The BaOH (BaOD) molecules were made in a Broida-type oven (12) by the reaction of barium metal vapor with a few mTorr of H_2O (D_2O). The metal was vaporized from an electrically heated alumina crucible and entrained in argon carrier gas. The total pressure in the oven was approximately 2 Torr.

The 6W output of a Coherent Innova 70 argon ion laser was used to pump two broadband (1 cm^{-1} bandwidth) dye lasers. One broadband dye laser, operated with Pyridine 2 dye, was used to excite the $^3P_1-^1S_0$ (7911 Å) atomic transition of barium to promote the production of BaOH (BaOD). The other broad band dye laser, operated with Styryl 9M dye, was scanned from 7900 to 8950 Å while the total fluorescence was recorded using a photomultiplier tube. This laser was chopped at about 1 kHz and the signal was detected with a lock-in amplifier.

After the laser excitation spectra were recorded, vibrational assignments were made with the help of dispersed laser-induced fluorescence. For these experiments the Styryl 9M dye laser (100–150 mW) was set on a particular bandhead and the laser-induced fluorescence was dispersed with a 0.64-m monochromator and detected with a cooled photomultiplier tube (RCA C31034) with photon counting electronics. Because of the extensive collisional relaxation observed under our experimental conditions, these dispersed fluorescence spectra were not very helpful.

RESULTS AND DISCUSSION

A. Electronic Transitions

Figures 1 and 2 are laser excitation spectra of BaOH and BaOD, respectively. The two main features at 8300 and 8714 Å are assigned to the two spin–orbit components of the $\tilde{A}^2\Pi-\tilde{X}^2\Sigma^+$ transition. The 000–000 band origins were estimated to be 12 045 ($^2\Pi_{3/2}$) and 11 476 ($^2\Pi_{1/2}$) for BaOH and 12 039 ($^2\Pi_{3/2}$) and 11 468 ($^2\Pi_{1/2}$) for
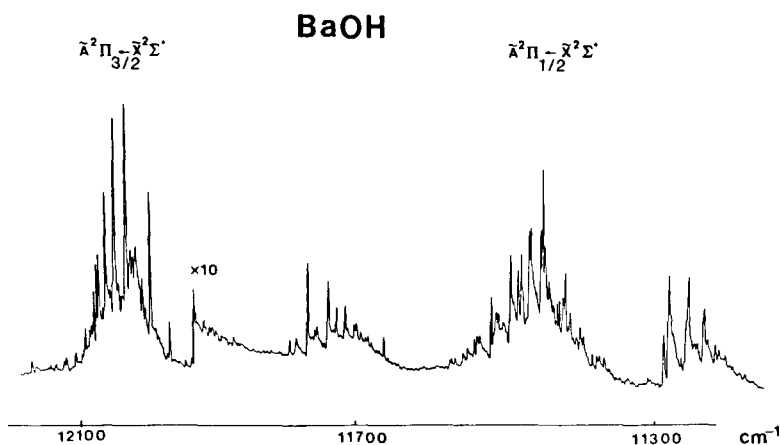

FIG. 1. BaOH laser excitation spectrum. The Styryl 9M broad band dye laser was scanned, and the total fluorescence was recorded. The $\tilde{A}^2\Pi_{3/2}-\tilde{X}^2\Sigma^+$ transition is recorded on a different intensity scale than the rest of the spectrum.

BaOD

FIG. 2. BaOD laser excitation spectrum. The Styryl 9M broad band dye laser was scanned, and the total fluorescence was recorded. The $\tilde{A}^2\Pi_{3/2}$–$\tilde{X}^2\Sigma^+$ transition is recorded on a different intensity scale than the rest of the spectrum.
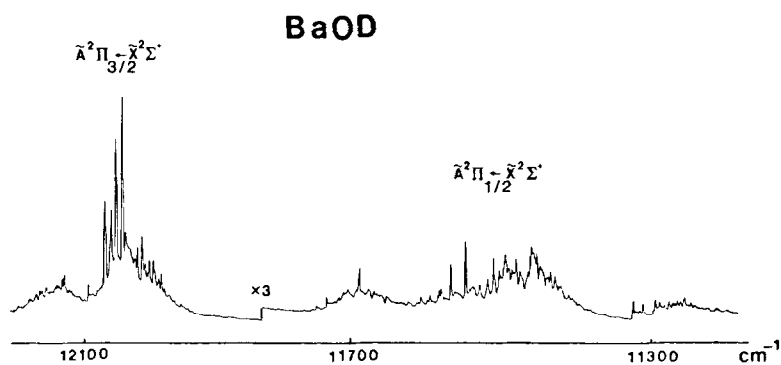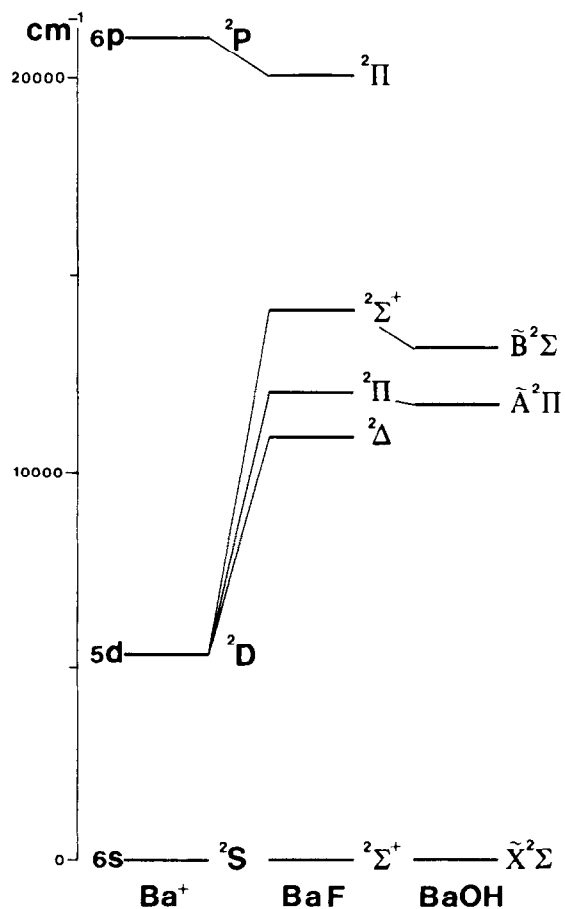

FIG. 3. Correlation diagram for Ba$^+$ perturbed by the linear OH$^-$ ligand. The positions of the electronic states of Ba$^+$, BaF, and BaOH are given for comparison.

BaOD with an error of about ± 2 cm^{-1}. The spin–orbit coupling constant A was found to be 570 ± 5 cm^{-1} which is similar to the A value (631 cm^{-1}) of BaF for the $A^2\Pi$ state (8).

The electronic states of BaOH arise from the Ba$^+$ ion perturbed by the OH$^-$ ligand. BaOH is linear in its ground state and excited states (1). The interaction of the OH$^-$ ligand causes the valence Ba$^+$ atomic orbitals to split and Fig. 3 shows the correlation between the valence Ba$^+$ atomic orbitals and the molecular orbitals of barium monohydroxide. The $\tilde{B}^2\Sigma^+$ and the $\tilde{A}^2\Pi$ excited states are $p\sigma$–$d\sigma$ and $p\pi$–$d\pi$ mixtures. Figure 3 also provides the ordering of the $^2\Delta$, $^2\Pi$, and $^2\Sigma^+$ excited states for BaF, which is isoelectronic with BaOH, and has been well studied ($8, 13, 14$). The $^2\Delta$ state is predicted to be above the $\tilde{B}^2\Sigma$ state for CaOH (15). The similarity of the spectra of the barium monofluoride and barium monohydroxide was used to interpret the BaOH and BaOD spectra.

According to the energy level diagram, the lowest-energy electric dipole allowed transition is $\tilde{A}^2\Pi$–$\tilde{X}^2\Sigma^+$, since the $^2\Delta$–$^2\Sigma^+$ electronic transition is electric dipole forbidden. However, the $^2\Delta$–$^2\Sigma^+$ transition can occur through vibronic coupling and off-diagonal spin–orbit mixing of the various components of the d-complex. For example both $A^2\Delta_{5/2}$–$X^2\Sigma^+$ and $A^2\Delta_{3/2}$–$X^2\Sigma^+$ transitions were observed for BaH (10).

We assign the bands near 8500 and 8850 Å to the $\tilde{A}'^2\Delta_{5/2}$–$\tilde{X}^2\Sigma^+$ transition. The vibrational assignments of these bands are ambiguous but we favor 000–000 for the $\tilde{A}'^2\Delta_{5/2}$–$\tilde{X}^2\Sigma^+$ transition at 8844 Å for BaOH and 8860 Å for BaOD.
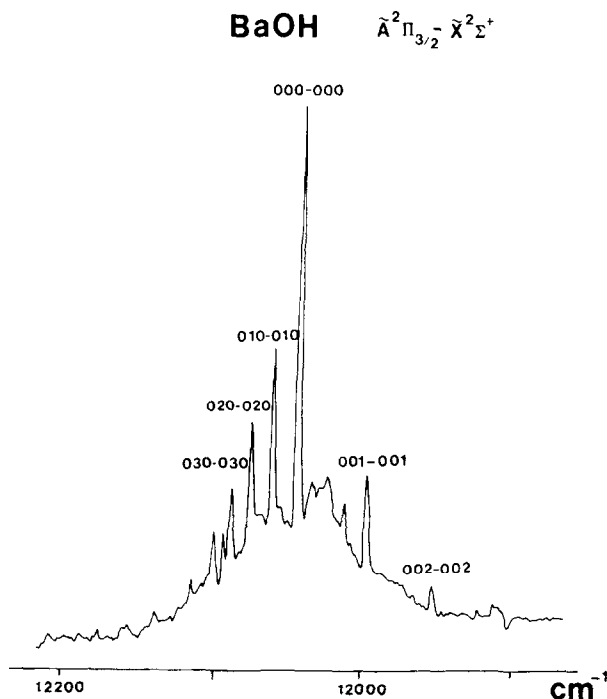

FIG. 4. Vibrational assignments of the $\tilde{A}^2\Pi_{3/2}$–$\tilde{X}^2\Sigma^+$ transition of BaOH.

B. Vibrational Analysis

There are three vibrational modes for the linear triatomic molecule BaOH: the O–H stretch (ν_1), the Ba–O–H bend (ν_2), which is doubly degenerate, and the Ba–O stretch (ν_3). The Franck–Condon factors favor the intensities of the vibronic bands which are associated with the metal atom vibrations, since the electronic transitions occur between orbitals which are centered on the metal atom. Therefore, ν_2 and ν_3 bands are expected in the spectra. Moreover the ν_1 mode at ~ 3600 cm^{-1} is not likely to be populated under the conditions of our experiment.

An attempt was made to assign as many bands as possible to activity in ν_3 and ν_2. Figures 4 and 5 show the vibrational assignments for the $\tilde{A}^2\Pi_{3/2}$–$\tilde{X}^2\Sigma^+$ spin components for BaOH and BaOD, respectively. The results of the bandhead analysis are listed in Tables I and II. These band heads are measured with an accuracy of about ±2 Å.

Figure 6 shows a resolved fluorescence scan of BaOH with the laser exciting the 000–000 band of the $\tilde{A}^2\Pi_{3/2}$–$\tilde{X}^2\Sigma^+$ transition. It is very hard to see the 000–001 band in the spectrum, since it occurs near the vicinity of the $\tilde{A}^2\Pi_{1/2}$–$\tilde{X}^2\Sigma^+$ system and the
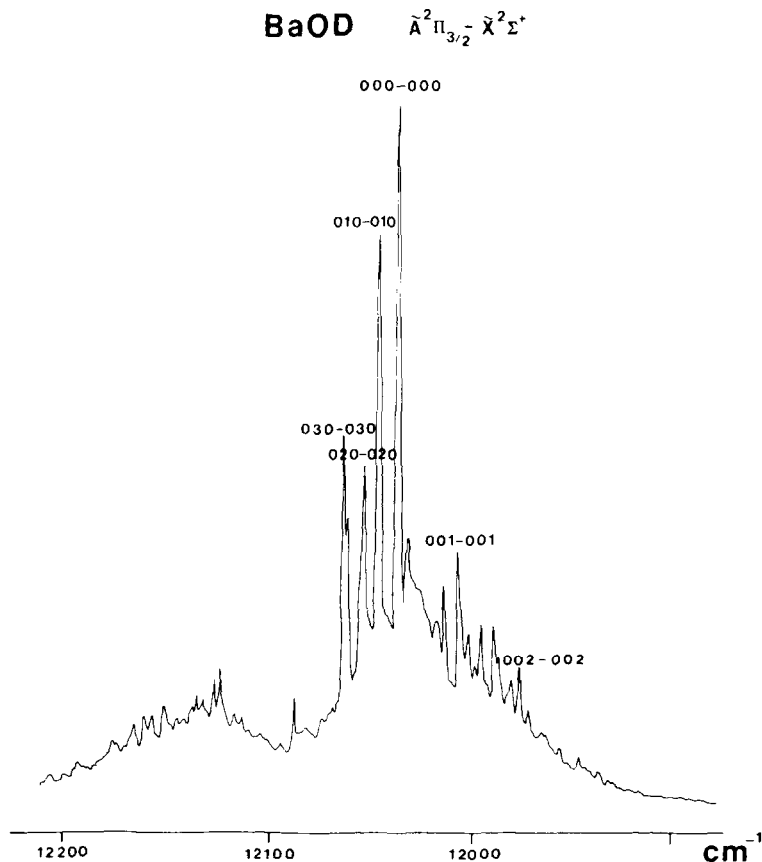

FIG. 5. Vibrational assignments of the $\tilde{A}^2\Pi_{3/2}$–$\tilde{X}^2\Sigma^+$ transition of BaOD.

TABLE I

Bandheads for the $\tilde{A}^2\Pi-\tilde{X}^2\Sigma^+$ Transition of BaOH and BaOD (in Å)

	$\tilde{A}^2\Pi_{3/2}-\tilde{X}^2\Sigma^+$				$\tilde{A}^2\Pi_{1/2}-\tilde{X}^2\Sigma^+$			
assignment	v=0	1	2	3	0	1	2	3
				BaOH				
0v0-0v0	8300	8292	8285	8278	8714	8704	8695	8685
00v-00v	8300	8324	8347		8714	8739		
				BaOD				
0v0-0v0	8304	8298	8294	8286	8718	8712	8706	8701
00v-00v	8304	8327	8348		8718	8731	8749	8774

$\tilde{A}^2\Pi_{1/2}$ state is populated by collisions. The BaOH emission spectra are greatly complicated by emission from collisionally populated levels. The presence of numerous perturbations facilitates these relaxation processes.

Since the ground state vibrational frequencies are known, it is possible to extract estimates for the excited state vibrational frequencies from the observed sequence structure. The spectra are reasonably consistent with $\nu_3' < \nu_3''$ and $\nu_2' > \nu_2''$ for both $\tilde{A}^2\Pi-\tilde{X}^2\Sigma^+$ and $\tilde{A}'^2\Delta-\tilde{X}^2\Sigma^+$ transitions. Therefore, the $00\nu_3'-00\nu_3''$ sequence structure proceeds to the red while the $0\nu_2'0-0\nu_2''0$ sequence structure proceeds slowly to the blue (Figs. 4 and 5). The $\tilde{B}^2\Sigma^+-\tilde{X}^2\Sigma^+$ transitions of BaOH and BaOD display similar sequence structure patterns. For the $\tilde{A}'^2\Delta - \tilde{X}^2\Sigma^+$ transition only one sequence was resolved, presumably the $00\nu_3'-00\nu_3''$ sequence, and $\nu_2' \approx \nu_2''$. Table III gives the known vibrational frequencies for BaOH and BaOD. As usual, changes in the head–origin separations as well as the effect of perturbations introduce considerable uncertainty (at least ± 10 cm^{-1}) in these measurements.

TABLE II

Bandheads for the $\tilde{A}'^2\Delta_{5/2}-\tilde{X}^2\Sigma^+$ Transition of BaOH and BaOD (in Å)

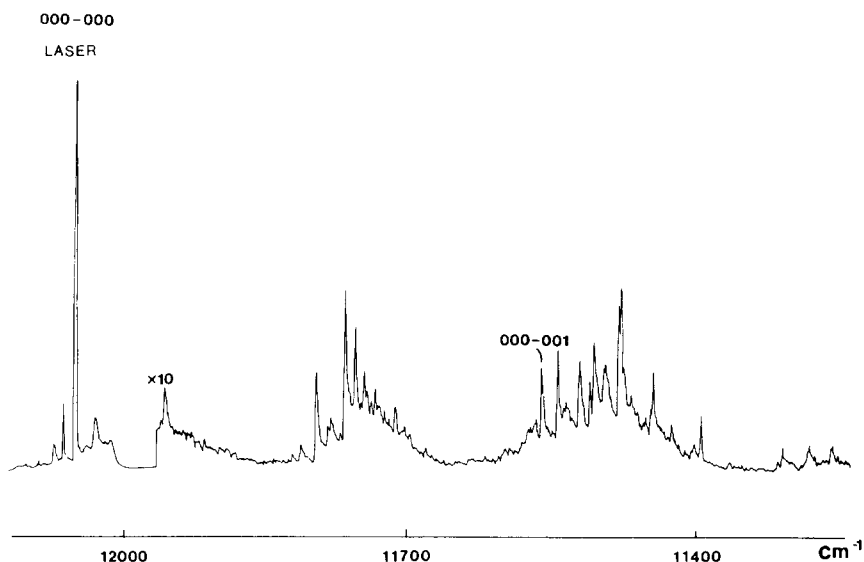| assignment	v=0	1	2
	BaOH		
00v-00v	8844	8864	8880
00v+1-00v	8484	8507	8516
	BaOD		
00v-00v	8860	8870	8883

FIG. 6. The resolved fluorescence spectrum of BaOH. One dye laser is tuned to the $^3P_1-{}^1S_0$ atomic transition of Ba (7911 Å). The monochromator was scanned with the second dye laser on the 000–000 band of the $\tilde{A}^2\Pi_{3/2}-\tilde{X}^2\Sigma^+$ transition at 8300 Å.

The assignment of the 000–000 band in the $\tilde{A}^2\Pi_{3/2}-\tilde{X}^2\Sigma^+$ transition was easier than in the more perturbed $\tilde{A}^2\Pi_{1/2}-\tilde{X}^2\Sigma^+$ transition. For the $\tilde{A}'^2\Delta-\tilde{X}^2\Sigma^+$ transition the absolute vibrational assignment is also uncertain because the red limit of the GaAs photomultiplier tube and the Styryl 9M dye was 9000 Å. By analogy with the corresponding $A'^2\Delta-\tilde{X}^2\Sigma^+$ transition of BaF, this means that much of the $\tilde{A}'^2\Delta-\tilde{X}^2\Sigma^+$ transition lies just beyond the red limit of our experiments.

The $\tilde{A}'^2\Delta_{5/2}-\tilde{X}^2\Sigma^+$ band near 8850 Å shows a small isotope shift of about 20 cm^{-1}. This shift is clearly too small for a vibronic transition involving a bending mode but consistent with a Ba–O stretching mode. However, the off-diagonal vibronic transitions involving stretching modes have relatively small intensities so this assignment is unlikely. The transition at 8840 Å is, therefore, most likely a 000–000 band. Comparison with BaF suggests that the bands near 8850 Å must be $\tilde{A}'^2\Delta_{5/2}-\tilde{X}^2\Sigma^+$ bands induced by off-diagonal spin–orbit mixing in the $\tilde{B}$, $\tilde{A}$, $\tilde{A}'$ d-complex.

TABLE III

Vibrational Frequencies for BaOH and BaOD (in cm^{-1})

	$\tilde{X}^2\Sigma^+$		$\tilde{A}^2\Pi$		$\tilde{A}'^2\Delta$	
	BaOH	BaOD	BaOH	BaOD	BaOH	BaOD
ν_2	342[a]	258[a]	352	268	342	258
ν_3	492[a]	482[a]	458	451	468	469

[a] values from ref.(1)

In BaOH the bands near 8500 Å, which lie between the $\tilde{A}^2\Pi_{3/2}-\tilde{X}^2\Sigma^+$ and $\tilde{A}^2\Pi_{1/2}-\tilde{X}^2\Sigma^+$ transitions (Fig. 1), are best assigned as the $\Delta v_3 = 1$ stretching sequence of the $\tilde{A}'^2\Delta_{5/2}-\tilde{X}^2\Sigma^+$ transition consistent with a $v'_3 = 480$ cm^{-1}. The corresponding transitions of BaOD near 8500 Å are probably better assigned to the $\Delta v_2 = 1$ sequence (i.e., 010–000, etc.) of the $\tilde{A}^2\Pi_{1/2}-\tilde{X}^2\Sigma^1$ transition consistent with $v'_2 = 261$ cm^{-1}. As was previously observed in the $\tilde{B}^2\Sigma^+-\tilde{X}^2\Sigma^+$ transition spin–orbit vibronic coupling allows the breakdown of the $\Delta v_2 = 2$ selection rule. This difference in the appearance of the BaOH and BaOD spectra near 8500 Å indicates the presence of numerous vibronic as well as electronic perturbations.

The reason for our $\tilde{A}-\tilde{X}$ misassignments in the previous BaOH/BaOD analysis is now clear (1). In that paper we analyzed what we believed to be $\tilde{B}-\tilde{A}-\tilde{X}$ cascade emission. In fact two types of $\tilde{A}-\tilde{X}$ emission are observed when the $\tilde{B}-\tilde{X}$ transition is excited. There is the dominant messy, collisionally induced $\tilde{A}-\tilde{X}$ emission (assigned in this report) and there is a simple, resonant high-v $\tilde{A}-\tilde{X}$ sequence band emission facilitated by $\tilde{B}-\tilde{A}$ perturbations. We misassigned this latter, perturbation-induced emission as $\tilde{B}-\tilde{A}-\tilde{X}$ cascade emission.

CONCLUSION

A preliminary low-resolution vibrational analysis of the $\tilde{A}^2\Pi-\tilde{X}^2\Sigma^+$ transitions of BaOH and BaOD is presented. There is evidence for the $\tilde{A}'^2\Delta$ state but further work to the red of 9000 Å is necessary to locate the $\tilde{A}'^2\Delta_{3/2}$ spin-component. The $\tilde{B}^2\Sigma^+$, $\tilde{A}^2\Pi$, and $\tilde{A}'^2\Delta$ states form a d-complex similar to the isoelectronic BaF molecule. The spectra display massive local and global perturbations among the members of this d-complex.

REFERENCES

1. S. KINSEY-NIELSEN, C. R. BRAZIER, AND P. F. BERNATH, J. Chem. Phys. 84, 698–708 (1986).
2. R. C. HILBORN, ZHU QINGSHI, AND D. O. HARRIS, J. Mol. Spectrosc. 97, 73–91 (1983).
3. P. F. BERNATH AND C. R. BRAZIER, Astrophys. J. 288, 373–376 (1985).
4. J. NAKAGAWA, R. F. WORMSBECHER, AND D. O. HARRIS, J. Mol. Spectrosc. 97, 37–64 (1983).
5. C. R. BRAZIER AND P. F. BERNATH, J. Mol. Spectrosc. 114, 163–173 (1985).
6. H. MARTIN AND P. ROYEN, Chem. Phys. Lett. 97, 127–129 (1983).
7. M. DOUAY, C. BRAZIER, AND P. F. BERNATH, unpublished results.
8. R. F. BARROW, A. BERNARD, C. EFFANTIN, J. D'INCAN, G. FABRE, A. EL HACHIMI, R. STRINGAT, AND J. VERGES, Chem. Phys. Lett. 147, 535–537 (1988).
9. L. VESETH, Mol. Phys. 25, 333–344 (1973).
10. A. BERNARD, C. EFFANTIN, J. D'INCAN, G. FABRE, R. STRINGAT, AND R. F. BARROW, Mol. Phys. 67, 1–18 (1989).
11. C. ALCARAZ, J. M. MESTDAGH, P. MEYNADIER, P. DE PUJO, J. P. VISTICOT, A. BINET, AND J. CUVELLIER, Chem. Phys. Lett. 156, 191–196 (1989), and personal communication J. P. Visticot and T. Gustavsson.
12. J. B. WEST, R. S. BRADFORD, J. D. EVERSOLE, AND C. R. JONES, Rev. Sci. Instrum. 46, 164–168 (1975).
13. R. F. BARROW, M. W. BASTIN, AND B. LONGBOROUGH, Proc. Phys. Soc. (London) 79, 518 (1967).
14. P. C. F. IP, P. F. BERNATH, AND R. W. FIELD, J. Mol. Spectrosc. 89, 53–61 (1981).
15. V. ORTIZ, J. Chem. Phys. 92, 6728–6731 (1990).